

Absorption spectrum analysis of uranium trichloride heptahydrate

M. Karbowiak^a, J. Drożdżyński^{a,*}, Z. Gajek^b

^aFaculty of Chemistry, University of Wrocław, ul. F. Joliot-Curie 14, 50-383 Wrocław, Poland

^bW. Trzebiatowski Institute of Low Temperature and Structure Research, Polish Academy of Sciences, P.O. Box 937, Wrocław, Poland

Abstract

A good quality absorption spectrum of a powdered sample of $\text{UCl}_3 \cdot 7\text{H}_2\text{O}$ was obtained at 4.2 K in the $4000\text{--}30\,000\text{ cm}^{-1}$ range. Analysis of the spectrum enabled the determination of the crystal-field parameters and assignment of 94 crystal-field levels. The energies of the levels were computed by applying a simplified angular overlap model as well as a semi-empirical Hamiltonian representing the combined atomic and crystal-field interactions. © 2001 Elsevier Science B.V. All rights reserved

Keywords: Uranium trichloride heptahydrate; Uranium(3+); Absorption spectra; Crystal-field analysis

1. Introduction

This paper presents a crystal-field level analysis performed on the basis of the low-temperature absorption spectrum of polycrystalline samples of $\text{UCl}_3 \cdot 7\text{H}_2\text{O}$. Spectroscopic crystal-field studies of trivalent uranium, due to experimental difficulties, have so far been exclusively carried out on single-crystal hosts of simple and complex lanthanide halides [1–10] and a polycrystalline $\text{U}(\text{HCOO})_3$ sample [11]. Most of these investigations, however, exhibit a substantial drawback depending on the appearance of strong, Laporte-allowed f–d bands in the spectra at energies as low as about $16\,000\text{--}18\,000\text{ cm}^{-1}$. As a result, the energy level structure of U^{3+} in different environments is relatively well established in the $0\text{--}16\,500\text{ cm}^{-1}$ region only. Hence, we turned our attention to uranium(III) compounds in polycrystalline form, for which good quality absorption spectra could also be recorded in the $15\,000\text{--}30\,000\text{ cm}^{-1}$ range.

2. Experimental

The compound was prepared according to the procedures reported in Ref. [12]. The electronic absorption spectrum of a thin film of the compound was recorded on a

Cary 5 NIR–Vis–UV spectrophotometer in the $4000\text{--}30\,000\text{ cm}^{-1}$ range. In order to obtain the spectrum, a well-ground mixture of the compound with some chlorinated naphthalene oil (refraction index 1.635) was placed between two quartz windows, approximately 0.8 cm in diameter, pressed to obtain a transparent layer, and placed in the cell compartment of an Oxford Instruments Model CF1204 cryostat. The spectrum was recorded at 4.2 and 300 K.

3. Parameterization of the crystal-field potential

Since no qualitative differences were found [12] between the X-ray powder diffraction data of $\text{UCl}_3 \cdot 7\text{H}_2\text{O}$ and $\text{LaCl}_3 \cdot 7\text{H}_2\text{O}$ it was assumed that these compounds are isostructural and form similar $[(\text{H}_2\text{O})_7\text{Me}(\text{Cl})\text{Me}(\text{H}_2\text{O})_7]\text{Cl}_4$ dimers, where $\text{Me}=\text{U}$ or La . The coordination polyhedron approximates two single-capped square antiprisms which share an equatorial edge formed by the bridging chloride atoms [13]. The other four chloride atoms are not bound to the metal ion. The cells are triclinic with space group $P\bar{1}$. Due to the lack of symmetry elements at the metal site in the compound under consideration as many as 27 independent crystal-field parameters describe the crystal-field (CF) potential. Preliminary estimation of their values is difficult in view of the fact that the first coordination sphere, being of major importance for the CF effect, is especially complex [12,13]. All ligands, i.e. the two chlorine ions and seven oxygens, are non-equivalent in the sense that any two of

*Corresponding author. Tel.: +48-71-320-4333; fax: +48-71-328-2348.

E-mail address: jd@wchuwr.chem.uni.wroc.pl (J. Drożdżyński).

them cannot be interchanged by a rotation only, leaving the system invariant. To simplify the phenomenological description of the system, the angular overlap model (AOM) [14], known to be especially efficient in cases of low-symmetry systems (see, for example, Ref. [15]), was applied. In this model the CF potential V is partitioned into certain spatial contributions attributed to ligands. The usual B_q^k CF parameters are then expressed in terms of the so-called intrinsic e_μ^t parameters, which correspond to the above-mentioned contributions and the specific $W_{kq}^{\mu t}$ factors, which depend on the geometry of the metal ion surroundings:

$$B_q^k = \sum_t \sum_\mu W_{kq}^{\mu t} e_\mu^t \quad (1)$$

The index t identifies ligands and μ represents the absolute value of the magnetic quantum number of a 5f electron in the local coordination system, taking values of 0, 1, 2, denoted also by σ , π , δ . Thus there are three e_μ^t AOM parameters per ligand. The total number of AOM parameters depends on the number of non-equivalent ligands, being equal to 27 (3×9) for the considered hydrate. The characteristic properties of the AOM parameters allow one to reduce the number of independent parameters to a few only. We fixed the metal–ligand distance dependence of the parameters in the form

$$e_\mu^t = e_\mu^0 \left(\frac{R_0}{R_t} \right)^{\alpha_\mu} \quad (2)$$

as well as the ratios between them, using the α_μ exponents in the above formula and the $e_\mu^t/e_{\mu'}^{t'}$ ratios from Ref. [15]. The $W_{kq}^{\mu t}$ coefficients were calculated on the basis of the crystallographic (X-ray) data reported in Ref. [13] for isostructural $\text{PrCl}_3 \cdot 7\text{H}_2\text{O}$.

The parameterization is a quite severe simplification in the cases of systems containing water molecules [16]. Nevertheless, this exceptionally compact description of the intricate CF potential is practically indispensable in the initial steps of the interpretation of complex spectra. Moreover, despite the apparent shortcomings, the model has been shown to work quite satisfactorily for hydrates [16].

4. Phases of interpretation

The fitting procedure was divided into a number of steps, starting from a raw single-parameter AOM approach to the standard CF Hamiltonian. In the first step of the calculations we only took into account crystal-field levels which could be assigned unambiguously. The remaining levels were gradually identified and included in the fitting procedure as the calculations proceeded. The initial values of the AOM parameters and their ratios were taken from the above ab initio calculations. In this calculation step a

single-parameter approximation was introduced through the following constraints:

1. $e_\delta^0 = e_\delta^{\text{Cl}} = 0$;
2. $e_\pi^0 = 0.363e_o^0$, $e_\pi^{\text{Cl}} = 0.339e_o^{\text{Cl}}$;
3. $e_o^{\text{Cl}} = 0.67e_o^0$

The e_o^0 and e_μ^{Cl} parameters are defined as averaged quantities over all ligands of a given type, with weights determined from the ab initio calculations. According to the above equations, e_o^0 becomes the only free parameter to be varied in the first step of the fitting procedure. The initial value of the e_o^0 parameter was estimated at 800 cm^{-1} .

In the second step, constraint 3 was relaxed and the two e_o^0 and e_o^{Cl} parameters, which separately describe the U–Cl and U–O interactions, were freely varied. In the next step, we released the e_o^0 and e_o^{Cl} parameters with the initial values obtained from the second step as well as the e_δ^0 and e_δ^{Cl} parameters with the starting value equal to 0. Constraints 2 were still maintained. Since the release of the e_δ^{Cl} parameter resulted in a parameter value different from the calculated value, this parameter was not included in further fitting procedures. In the final AOM phase the e_σ^0 , e_π^0 , e_δ^0 , e_σ^{Cl} and e_π^{Cl} parameters were treated as independent variables with the initial values of e_σ^0 and e_π^{Cl} determined from the third step and those of e_π^0 and e_π^{Cl} from the relation in constraint 2. The final values of the AOM parameters (Table 1) were determined with a relatively small error and were consistent with the applied model. At this stage the largest difference between the computed and experimental crystal-field levels did not exceed 122 cm^{-1} and the r.m.s error was 42.6 cm^{-1} .

However, since the applied conventional AOM approach does not precisely reflect the polarization effects, which are expected to be important for the investigated compound, we switched to the B_q^k parameterization. Thus, in the next steps of the fitting procedure, all the usual CF parameters were varied paying special attention to the B_q^2 parameters, which are especially sensitive to the electric polarization of the surroundings. Their initial values were determined according to Eq. (1) from the obtained AOM parameters listed in Table 1. In the next two steps we released the crystal-field parameters with the largest absolute values, i.e. the B_1^6 , $\text{Im } B_2^6$, B_4^6 , $\text{Im } B_4^6$, $\text{Im } B_5^6$ and B_0^2 , $\text{Im } B_1^2$, B_2^2 , $\text{Im } B_2^2$ parameters, respectively. At this stage of the calculations, all computed values exhibit relatively small changes and parameter errors. In the final fit, seven ‘free

Table 1
AOM parameters (cm^{-1}) for $\text{UCl}_3 \cdot 7\text{H}_2\text{O}$

e_σ^{Cl}	e_σ^0	e_π^{Cl}	e_π^0	e_δ^{Cl}	e_δ^0
547 (92) ^a	1126 (86)	154 (81)	422 (78)	[0] ^b	111 (58)

^a Values in parentheses are parameter errors.

^b Parameters not varied in the fitting procedure.

Table 2

Free ion and crystal-field parameters for $\text{UCl}_3 \cdot 7\text{H}_2\text{O}$

Parameter ^{a,b}	(cm^{-1})	Parameter ^{a,b}	(cm^{-1})
E_{avg}	19 827 (17)	B_4^4	[374]
F^2	40 488 (58)	$\text{Im } B_4^4$	[−491]
F^4	32 544 (81)	B_0^6	[−130]
F^6	22 866 (75)	B_1^6	428 (90)
α	28 (5)	$\text{Im } B_1^6$	[−77]
β	−622 (35)	B_2^6	[171]
ζ	1622 (10)	$\text{Im } B_2^6$	133 [100]
B_0^2	−126 (76)	B_3^6	[−251]
B_1^2	[−109]	$\text{Im } B_3^6$	[−14]
$\text{Im } B_1^2$	−423 (47)	B_4^6	−489 (110)
B_2^2	−209 (53)	$\text{Im } B_4^6$	−1832 (81)
$\text{Im } B_2^2$	−350 (55)	B_5^6	[160]
B_0^4	188 (106)	$\text{Im } B_5^6$	1197 (96)
B_1^4	[−99]	B_6^6	−498 (98)
$\text{Im } B_1^4$	[−81]	$\text{Im } B_6^6$	−241 (91)
B_2^4	[−66]		
$\text{Im } B_2^4$	[−238]	σ^c	36
B_3^4	[136]	n	94
$\text{Im } B_3^4$	−529 (83)		

^a The values of the free ion parameters which were kept constant during the fitting procedures were: $\gamma = 1148$; $T^2 = 306$, $T^3 = 42$, $T^4 = 188$, $T^6 = -242$, $T^7 = 447$, $T^8 = 300$; $M^0 = 0.672$, $M^2 = 0.372$, $M^4 = 0.258$; $P^2 = 1216$, $P^4 = 608$, $P^6 = 122$.

^b Values in parentheses are parameter errors. Values of the crystal-field parameters in brackets were obtained by deconvolution of AOM parameters and were kept constant during the fitting procedures.

^c r.m.s. deviation: $\sigma = \sum [\Delta_i / (n - p)]^{1/2}$, where Δ_i is the difference between the observed and calculated energies, n is the number of levels fitted and p is the number of parameters freely varied.

ion' and 13 crystal-field parameters were varied simultaneously (Table 2). Relaxing of the remaining crystal-field parameters led either to large errors in the determination of parameter values or to large deviations from the initial values and usually also to larger r.m.s. errors.

5. Results and discussion

The absorption spectrum recorded at 4.2 K is presented in Figs. 1 and 2. The near-IR and visible part of the spectrum consists of relatively intense, sharp and well-separated absorption lines. The low site symmetry of U^{3+} results in the absence of distinct vibronic lines and the appearance of $(2J + 1)/2$ lines for each multiplet. Hence, the recorded lines may be assigned to transitions from the lowest component of the $^4\text{I}_{9/2}$ ground level to the components of the excited $^{2S+1}L_J$ multiplets. In addition to some very weak features of unknown origin, the observed number of lines does not exceed $(2J + 1)/2$, which is indicative of single uranium sites in the compound.

The conventional parametric Hamiltonian requires 26 real and imaginary B_q^k parameters. For such low site symmetries a least-square routine may lead to a false minimum of no physical meaning. To limit the space of the possible solutions we decided to apply the AOM con-

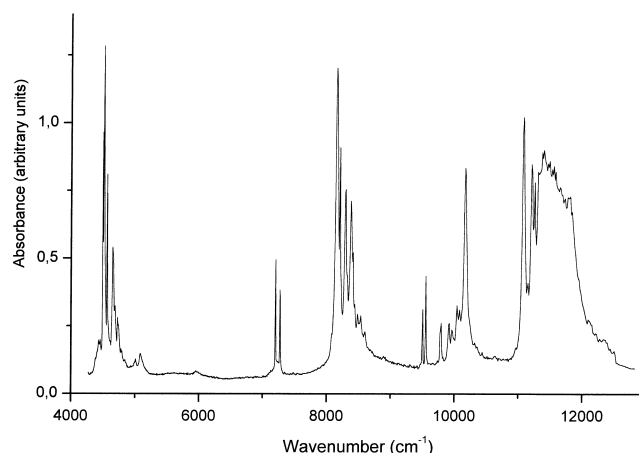


Fig. 1. Absorption spectrum of $\text{UCl}_3 \cdot 7\text{H}_2\text{O}$ at 4 K in the 4000–13 000 cm^{-1} range.

straints. In this phase of interpretation, we obtained somewhat larger r.m.s. errors, but the parameters retained their physical meaning.

In the calculations, seven 'free ion' and 13 crystal-field parameters were allowed to vary freely. As can be seen from Table 3 almost all absorption bands were recorded and assigned. In comparison with earlier analyses [1–11] the number of levels included in the calculations is larger. Finally, we could identify 94 crystal-field levels (Table 3).

The relatively small r.m.s. deviation of 36 cm^{-1} (Table 2) as well as the good relationship between the computed and theoretical parameters allowed us to conclude that the obtained values retained their physical meaning. To the best of our knowledge these are not only the first crystal-field calculations for such uranium(III) systems, but also one of the first for hydrated nf^N electron compounds of very low site symmetry.

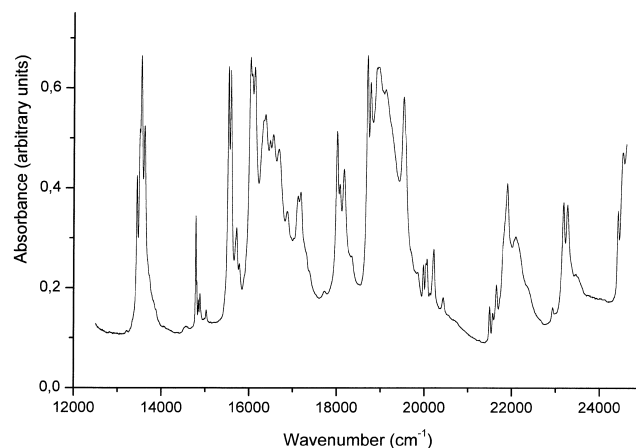


Fig. 2. Absorption spectrum of $\text{UCl}_3 \cdot 7\text{H}_2\text{O}$ at 4 K in the 13 000–25 000 cm^{-1} range.

Table 3
Calculated and experimental energy levels for $\text{UCl}_3 \cdot 7\text{H}_2\text{O}$

$^{2S+1}L_J^a$	Calculated energy (cm^{-1})	Experimental energy (cm^{-1})	$E_{\text{exp}} - E_{\text{calc.}}$ (cm^{-1})
$^4\text{I}_{9/2}$	21 167 329 546 704	0 170	–21 3
$^4\text{I}_{11/2}$	4455 4507 4576 4622 4724 4789	4494 4511 4561 4649 4686 4725	39 4 –15 –38 –38 –64
$^4\text{F}_{3/2}$	7177 7268	7198 7270	21 2
$^4\text{I}_{13/2}$	8098 8204 8260 8316 8440 8525 8604	8150 8202 8288 8376 8483 8530 8595	51 –2 28 60 43 5 –9
$^2\text{H}_{29/2}$	9538 9604 9753 9881 9941	9506 9551 9794 9915 9962	–32 –53 41 34 21
$^4\text{F}_{5/2}$	10 020 10 083 10 144	10 038 10 080 10 165	18 –3 21
$^4\text{S}_{3/2} + ^4\text{G}_{5/2} + ^4\text{F}_{7/2} + ^4\text{I}_{15/2}$	11 039 11 140 11 188 11 245 11 397 11 433 11 488 11 548 11 627 11 672 11 737 11 788 11 873 11 999 12 118 12 268 12 365	11 072 11 142 11 200 11 246 11 309 11 379 11 457 11 551 11 659 11 778 11 960 12 116 12 221 12 348	33 2 12 1 –88 –54 –31 3 –13 –10 –39 –2 –47 –17
$^4\text{G}_{7/2}$	13 482 13 582 13 630 13 754	13 441 13 539 13 613 13 724	–41 –43 –17 –30
$^4\text{F}_{9/2}$	14 725 14 787 14 811 14 871 14 968	14 785 14 808 14 844 14 880 15 020	60 21 33 9 52
$^2\text{H}_{211/2}$	15 463 15 543 15 584 15 674 15 744 15 879	15 522 15 577 15 711 15 774 15 883	–22 –7 37 30 4
$^2\text{K}_{13/2} + ^4\text{D}_{3/2} + ^4\text{D}_{1/2}$	16 038 16 107 16 170 16 273 16 310 16 363 16 426 16 512 16 688 16 920	16 021 16 062 16 120 16 319 16 367 16 471 16 544 16 670 16 868	–17 –45 –50 9 4 45 32 –18 –52

Table 3. Continued

$^{2S+1}L_J^a$	Calculated energy (cm^{-1})	Experimental energy (cm^{-1})	$E_{\text{exp}} - E_{\text{calc.}}$ (cm^{-1})
$^2\text{G}_{17/2} + ^4\text{G}_{9/2}$	16 972 17 029 17 089 17 114 17 193 17 245 17 271 17 382 17 510	16 952 17 017 17 109 17 170 17 251 17 298 17 371	–21 –12 –5 –23 5 27 –11
$^4\text{D}_{5/2}$	17 945 18 030 18 162	18 002 18 064 18 159	55 34 –3
$^2\text{L}_{15/2} + ^4\text{D}_{3/2}$	18 653 18 744 18 834 18 921 19 070 19 116 19 202 19 359 19 470 19 513	18 694 18 762 18 834 18 935 19 105	40 18 14 –11
$^2\text{H}_{111/2}$	19 934 19 977 20 028 20 067 20 100 20 143	19 972 20 030 20 054 20 122 20 209	–5 2 –13 22 66
$^2\text{D}_{15/2}$	20 496 20 650 20 764	20 422	–74
$^2\text{G}_{19/2} + ^2\text{I}_{11/2} + ^2\text{P}_{1/2}$	21 389 21 467 21 569 21 640 21 753 21 789 21 878 21 941 22 026 22 084 22 239 22 378	21 486 21 564 21 641 21 888 22 082 22 382	19 –6 1 10 –2 4
$^4\text{D}_{7/2} + ^2\text{D}_{3/2}$	22 675 22 897 23 019 23 079 23 179 23 264	22 934 23 174 23 259	37 –5 –5
$^2\text{I}_{13/2} + ^2\text{L}_{15/2} + ^2\text{H}_{19/2} + ^2\text{F}_{5/2}$	24 453 24 571 24 660 24 683	24 414 24 512	–39 –60

^a Nominal quantum numbers for the atomic state associated with the group.

6. Conclusions

The obtained good-quality low-temperature absorption spectrum of a powdered sample of $\text{UCl}_3 \cdot 7\text{H}_2\text{O}$ enabled a successful crystal-field analysis in the 0–25 000 cm^{-1} absorption range. Compared with earlier analyses of other uranium(III) systems the number of levels included in the calculations is larger and the r.m.s. deviation is relatively small. The AOM model was found to be useful in the determination of the initial values for the B_q^k parameterization.

References

- [1] J. Drożdżyński, in: A.J. Freeman, C. Keller (Eds.), *Handbook on the Physics and Chemistry of the Actinides*, Vol. 6, Elsevier, 1991, p. 282.
- [2] H.M. Crosswhite, H. Crosswhite, W.T. Carnall, A.P. Paszek, J. Chem. Phys. 72 (1980) 5103.
- [3] W.T. Carnall, H.M. Crosswhite, ANL-84-90, Optical spectra and electronic structure of actinide ions in compounds and solutions, Argonne National Laboratory, 1985.
- [4] E. Simoni, M. Louis, J.Y. Gesland, S. Hubert, J. Lumin. 65 (1995) 153.
- [5] M. Karbowiak, K.M. Murdoch, J. Drożdżyński, N.M. Edelstein, S. Hubert, Acta Phys. Polon. A 90 (2) (1996) 371.
- [6] M. Karbowiak, E. Simoni, J. Drożdżyński, S. Hubert, Acta Phys. Polon. A 90 (2) (1996) 367.
- [7] H.P. Andres, K. Krämer, H.-U. Güdel, Phys. Rev. 54 (1996) 3830.
- [8] M. Karbowiak, J. Drożdżyński, K.M. Murdoch, N.M. Edelstein, S. Hubert, J. Chem. Phys. 106 (1997) 3067.
- [9] M. Karbowiak, J. Drożdżyński, S. Hubert, E. Simoni, W. Stręk, J. Chem. Phys. 108 (1998) 10181.
- [10] M. Karbowiak, N. Edelstein, Z. Gajek, J. Drożdżyński, Spectrochim. Acta A 54 (1998) 2035.
- [11] M. Karbowiak, J. Drożdżyński, J. Alloys Comp. 300/301 (2000) 329–333.
- [12] J. Drożdżyński, Inorg. Chim. Acta 109 (1985) 79.
- [13] A. Habenschuss, F.H. Spedding, Cryst. Struct. Comm. 7 (1978) 535.
- [14] Z. Gajek, J. Mulak, M. Faucher, J. Phys. Chem. Solids 48 (1987) 947.
- [15] Z. Gajek, J. Mulak, J. Phys. Condens. Matter 4 (1992) 427.
- [16] M. Karbowiak, Z. Gajek, J. Drożdżyński, Chem. Phys. 261 (2000) 301.